

Electronic Supplementary Information

Transamidation and decomposition of dimethylformamide during alkylammonium lead triiodide film formation for perovskite solar cells

Michael V. Lee, Sonia R. Raga, Yuichi Kato, Matthew R. Leyden, Luis K. Ono, Shenghao Wang, Yabing Qi*

Energy Materials and Surface Sciences Unit (EMSS), Okinawa Institute of Science and Technology Graduate University (OIST), 1919-1 Tancha, Onna-son, Kunigami-gun, Okinawa, Japan 904-0495

* Yabing.Qi@OIST.jp

Supplementary Information. Detailed experimental methods, and supplementary experimental results.

Table of Contents

Supplementary Results.....	3
Carbonylation and Decomposition	3
Absorption by UV-visible spectroscopy	8
Time-evolution of a Film with Excess MAI and DMF Upon Exposure to Air	10
In situ XRD During Annealing of a GB Closed Film Showing the Retention of the T Peak with Annealing.....	11
In Situ Annealing of a Solution-Deposited Film without DMF or Excess MAI	12
In Situ Annealing of a Vacuum-Deposited Film without Excess MAI	13
Reversible Annealing of a Vacuum-Deposited Film with Excess MAI	13
XRD Confirmation of Perovskite Structure and Orientation.....	15
Film Crystallinity and Peak Shifts	16
One Explanation for the T Phase XRD Peaks	19
Perovskites Prepared by Chemical Vapor Deposition	20
TOF-SIMS Depth Profiling	21
XRD of a Film Prepared by the Two-Step Solution Method Using PbI_2 and DMAI.....	22
References	23

Supplementary Results

Carbonylation and Decomposition

Carbonylation of lead by DMF and decomposition of DMF are reasonable reactions considering the composition of perovskite solutions. Both reactions can break the covalent C-N bond of DMF to form DMA and also formyl (CHO) or carbonyl (CO) fragments, any of which might then be incorporated into PSC films. Based on the presence of NMF in spite of its volatility, and on the XPS measurements in the manuscript and below, transamidation is the primary mechanism for producing DMA, but when air is present, carbonylation or decomposition also produce DMA.

In the preparation of some metal-organic frameworks, DMF reacts with rhodium, ruthenium, or iridium chloride to carbonylate the metal centers.^{1,2} The reaction is accelerated in the presence of water.¹ PbCl₂ or PbI₂, which are similar metal halides, could be carbonylated by DMF in a similar fashion when heated in the presence of water. Carbonylation introduces either carbonyl (CO) or formyl (HCO) ligands and adds another phase to the perovskite. Carbonylation also produces DMA. Alternatively, DMF could simply decompose. DMF decomposes by thermal cleavage of the N-CHO bond at 152 °C, when irradiated with visible light, or when catalyzed by TiO₂.²⁻⁴ Degradation would introduce DMA into perovskite films, as well as either carbonyl (CO) or formyl (HCO) groups.

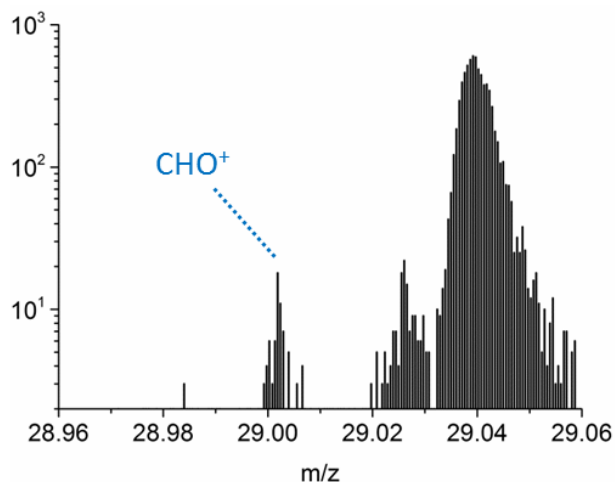


FIG. S1. TOF-SIMS of two-step perovskite film at $m/z=29.002$ for CHO^+ ion. The carbonyl ion is present, but the intensity is much lower than DMA.

Interestingly, we observed a weak peak ($m/z = 29.002$) for a CHO^+ ion (FIG. S1), which could be the other half of a DMF molecule. A CHO group would not be generally be volatile as it would be bound to the metal center. In contrast, NMF would be volatile as a free solvent molecule and would generally evaporate in vacuum without being observed. Because of the difference in intensity between DMA and CHO peaks, we believe transamidation is the main reaction introducing DMA. However the presence of CHO indicates that decomposition can still play a role. CO does not ionize as readily as CHO in mass spectrometry.⁵ Low signal from CHO^+ ions in TOF-SIMS suggests that either the level of $-\text{CHO}$ ligands is small, or the CHO^+ ions come from $-\text{CO}$ ligands that are more difficult to ionize. One might question whether DMF solvent molecules were trapped in the film and fragmented during analysis to produce DMA and CHO, but in that case the DMF peaks should be more prominent than DMA. In fact, the reverse is true: the primary ion peak for protonated $[\text{DMF}+\text{H}]^+$ ($m/z = 74.061$) is weaker than the $[\text{DMA}+\text{H}]^+$ peak by roughly two orders of magnitude (FIG. 2 and S2). The intensity is similar to that of NMF, however NMF is a volatile solvent and would be expected to evaporate in vacuum.

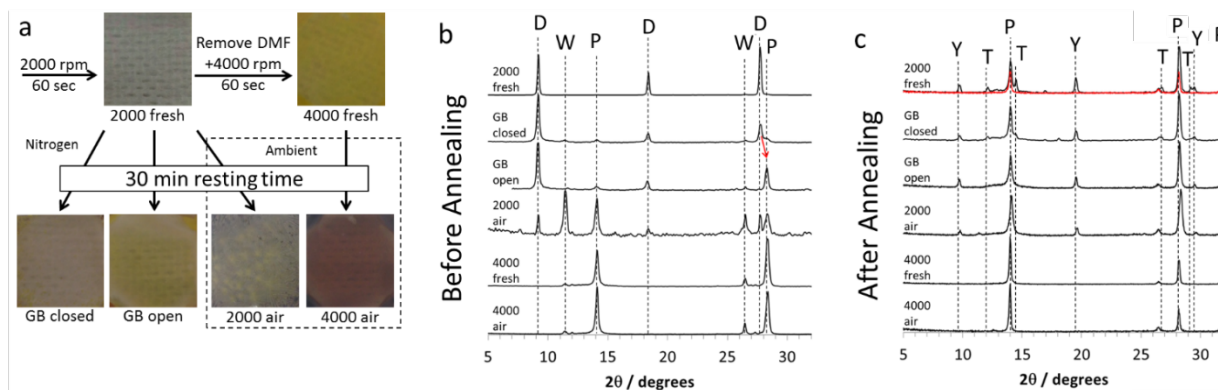


FIG. S2. Independent DMF-mediated and water-mediated processes compete to form perovskite with incorporated DMA. a) Graphical representation of the different conditions applied to understand the chemical and structural changes during annealing. Optical images of MAI-rich perovskite films after spin-coating but before annealing show dramatic differences based on treatment. Samples were spin-coated and then analyzed immediately, or after storage in a nitrogen glove box (GB), or after storage in air for 30 min to compare effects of DMF, exposure to TiO_2 , and exposure to air. XRD of films from b) before annealing and c) after annealing. The red line in c) shows the **2000 fresh** sample after additional annealing and is the same as in the main manuscript.

The DMF^*PbI_2 -complex peaks (D) include a peak at around 27.5° . In some instances this peak shifts to a higher angle of 18° that overlaps with the perovskite (220) peak (FIG. S2, **GB open**). In all instances where a D peak exists (with excess MAI) and samples are annealed in air, an additional set of peaks appears. If DMF were to carbonylate the Pb atoms either through direct carbonylation or as a result of decomposition of DMF, a new crystal phase would be expected. We have tentatively labeled the peaks with a “Y” to denote carbonylation. There are many crystal structures that include a carbonyl on a lead atom, so it would not be possible to identify this phase without separating it from the remaining content of the films.

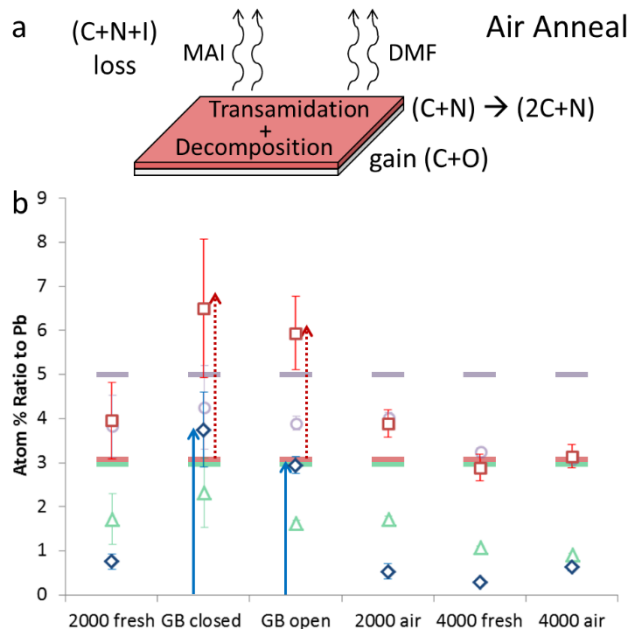


FIG. S3. Transamidation and MAI loss are observed by XPS in all cases, but decomposition to form CO or CHO is only observed if perovskite films are exposed to air. Decomposition of DMF adds a 1:1 ratio of C and O. For reference, solid horizontal purple, red, and green bars show the levels of iodine, carbon, and nitrogen in the initial 3:1 solution of MAI: PbI₂. Blue diamonds, red squares, green triangles, and purple circles represent atomic ratios relative to Pb 4*f* for O 1*s*, C 1*s*, N 1*s*, and I, respectively based on XPS fine scans for films annealed at 110 °C in air. Error bars represent standard deviation. Sample names refer to the treatment of the sample from Table 1 in the main text. Red dotted arrows and solid blue arrows in b) denote added oxygen and an equivalent amount of carbon. Annealing in air increases carbon and oxygen by equivalent amounts. If equivalent CO is subtracted in b), the results for annealing in air mirror those for annealing in nitrogen (main text, FIG. 5).

Air exposure inducing carbonylation is consistent with the XPS results after annealing in air (FIG. S3), in addition to the observation of CHO⁺ peaks in TOF-SIMS spectra (FIG. S1) and peak patterns observed in XRD spectra (FIG. S2). When samples are annealed in air, XPS measures significant oxygen content, whereas oxygen content is negligible after annealing in nitrogen. In cases where the increase is greatest, there is also a significant increase in carbon of similar magnitude. If equivalent ratios of carbon and oxygen are subtracted, the composition would be similar to those observed after annealing in air. The ratios would have carbon content roughly one carbon higher than the level of nitrogen. Nitrogen and iodine are reduced in equal

amounts from the starting ratios. Although complicated, the results are at least consistent with carbonylation or formylation of lead.

Absorption by UV-visible spectroscopy

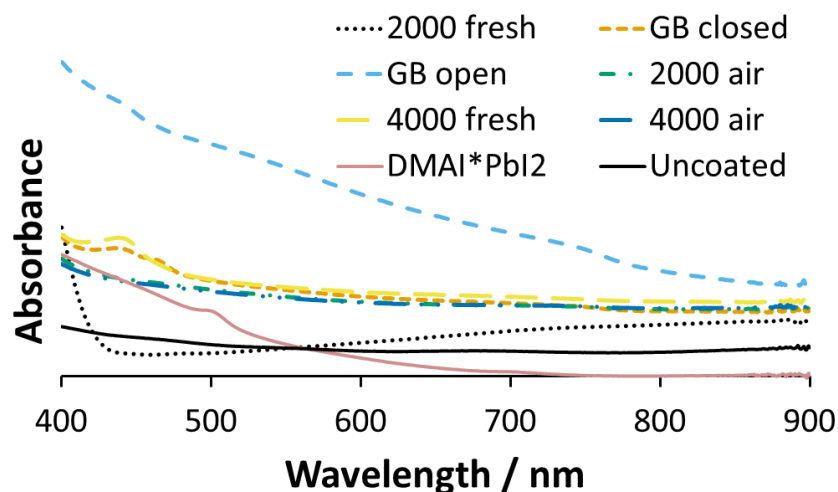


FIG. S4. UV-vis spectra from films prepared as presented in the main manuscript. Each spectrum was normalized individually. The **2000 fresh** sample was initially optically transparent, but over the course of a scan, the transparency decreased gradually approaching the spectrum of a sample after storage in air, **2000 air**.

The absorbance spectra show clear qualitative differences between films prepared and exposed to different conditions (FIG. S4). A freshly spin-coated film, **2000 fresh**, absorbs below 400 nm and the apparent absorbance is lower than that of the blank because of scattering from the rough surface of the blank. The scan time is on the order of 10 minutes, which is sufficient time for the P and W peaks to appear in a fresh sample. Over the course of the scan of the fresh film, the absorbance increases toward that of a film stored in air, **2000 air**. Although scattering and possible differences in thickness make it difficult to quantify the absorbance, the absorption cutoff and absorption peak variation are clear in most samples. Additional peaks are present in the samples prepared by storing in the glove box in a closed petri dish or with the excess DMF removed by faster spinning during deposition. The baseline is higher in the sample stored in the glove box in an open container. In each of the samples except the fresh one, the cutoff below 800

nm from perovskite absorption has begun to appear. To clearly present the differences in the manuscript, the spectra were normalized without subtracting the substrate background. The background is essentially flat across the measurement range, although scattering increases the apparent absorbance. The difference between the maximum absorption and the average value between 850-900 nm was normalized to 1, and the value of the value between 850-900 nm was maintained, since perovskite isn't expected to absorb in this region.

The optical bandgaps are similar, but also change depending on exposure conditions.. The bandgaps are all 1.58-1.60 eV, which is consistent with the literature. A film prepared with DMAI and PbI_2 has an absorption peak at 500 nm, and absorption that has a cutoff at 744 nm (1.67 eV).

Time-evolution of a Film with Excess MAI and DMF Upon Exposure to Air

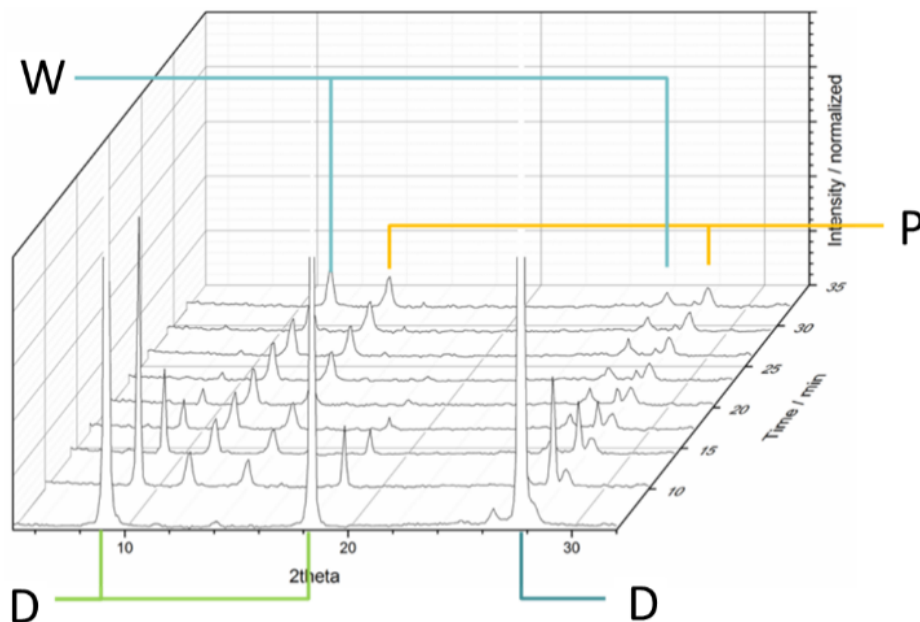


FIG. S5. Evolution of 2θ - θ XRD spectra of MAPbI_3 films with exposure to air. The P and W peaks appear in less than 10 minutes and increase slightly to stabilize after about 30 minutes. The D peaks gradually decrease in intensity and are mostly gone after 20 minutes in air. Decreasing D peaks appear to be only loosely correlated to the increase in P and W. Further into the page represents increasing time.

In situ XRD during air exposure (FIG. S5) shows the evolution between samples **2000 fresh** and **2000 air**. Air exposure leads to the emergence of the P and W peaks. Over time the D peaks decrease in intensity. The D peaks disappear as DMF evaporates. W peak positions agree with literature spectra for a water complex, $(\text{MA})_4\text{PbI}_6 \cdot 2\text{H}_2\text{O}$ and are consistent with water incorporation into the film. Although a 3:1 ratio of MAI:PbI₂ has excess MAI, it is less than the 4:1 ratio required for complete conversion to the water complex. A 1:2 ratio of MAPbI_3 to $(\text{MA})_4\text{PbI}_6 \cdot 2\text{H}_2\text{O}$ would use all of the MAI and PbI₂, while loss of MAI would move equilibrium between the two structures more toward the MAPbI_3 . This may be consistent with similar order of magnitudes for the P and W peaks.

In situ XRD During Annealing of a GB Closed Film Showing the Retention of the T Peak with Annealing

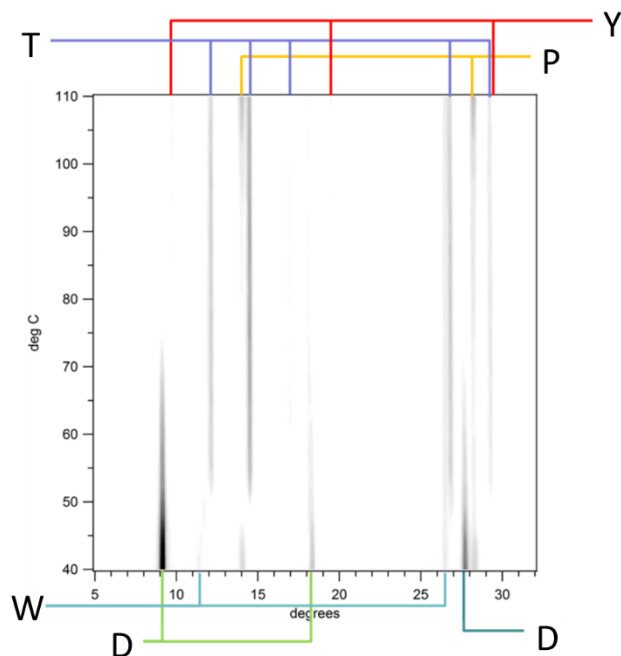


FIG. S6. *In situ* XRD on a film prepared at 2000 rpm and stored in a closed petri dish for 30 minutes before measuring, **GB closed**. During heating, peaks associated with DMF, i.e., D peaks, weaken and disappear. As the film is annealed above 45 °C and then 50 °C, the small peak at $2\theta = 11.5^\circ$ shifts to a higher angle in two steps to 12.1° . Similarly and simultaneously, the peak at 14.0° shifts up to 14.5° . This shift transforms the P + W peaks into the T structure peaks. The horizontal axis is 2θ degrees from XRD, while the vertical axis is temperature in °C, and the value indicates the intensity of the XRD line (dark = more intense).

For a sample that was stored in a closed petri dish in a glove box prior to analysis (FIG. S6), similar trends are observed as for samples that were annealed fresh. However, the shifted D peak can also be observed. Although most of the DMF evaporates with mild heating, D peaks are still present and gradually decrease in intensity during annealing until the P peaks reappear in the transition at 85-95 °C. At around 40-55 °C, the transition from P + W to T is also observed. Surprisingly, when the P and W peaks shift, some intensity remains unchanged at the (220) perovskite peak position. This cannot be from the P perovskite structure because no (110) peak

remains. Excess signal in the (220) peak position can be from a shifted D peak from a DMF-related structure.

In Situ Annealing of a Solution-Deposited Film without DMF or Excess MAI

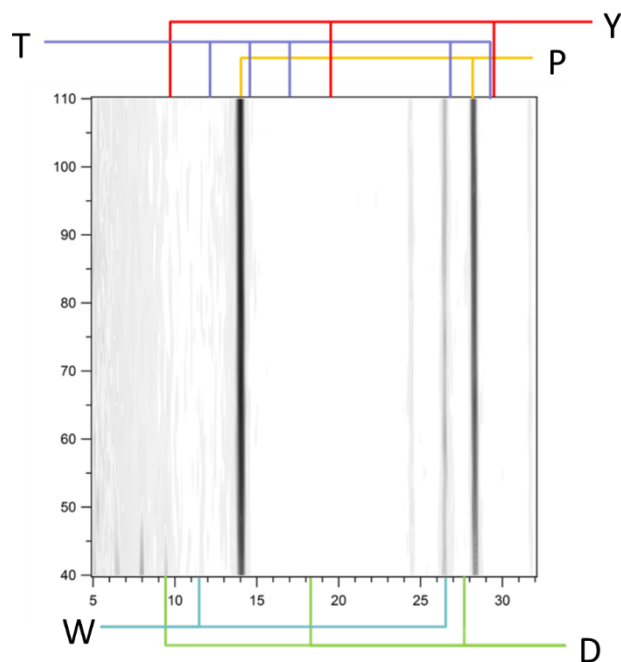


FIG. S7. A solution-prepared film without excess MAI has the perovskite spectrum throughout annealing. A film prepared fresh at 2000 rpm using a 1:1.25 ratio of PbI_2 : MAI was annealed measured directly following preparation. Without excess methylammonium halide, less DMF is retained after spin-coating. The P peaks from the perovskite structure are already present. Initially there are also three peaks below 10 degrees that were not present with excess MAI. No T peaks are observed without excess MAI. After the film temperature reaches 50 °C, only the perovskite peaks remain. The horizontal axis is 2θ degrees from XRD, while the vertical axis is temperature in °C, and the value indicates the intensity of the XRD line (dark = more intense).

When films are prepared without excess MAI and analyzed by *in situ* XRD (FIG. S7), then the $(\text{MA})_4\text{PbI}_6 \cdot 2\text{H}_2\text{O}$ structure doesn't form. The concerted shifts of the P and W peaks to form the T peaks are also not observed. Perhaps perovskites are more stable against water incorporation when excess MAI was not added or after it has been removed. Non-crystalline components might still absorb water. Interestingly, three new peaks are present below 10 degrees.

In Situ Annealing of a Vacuum-Deposited Film without Excess MAI

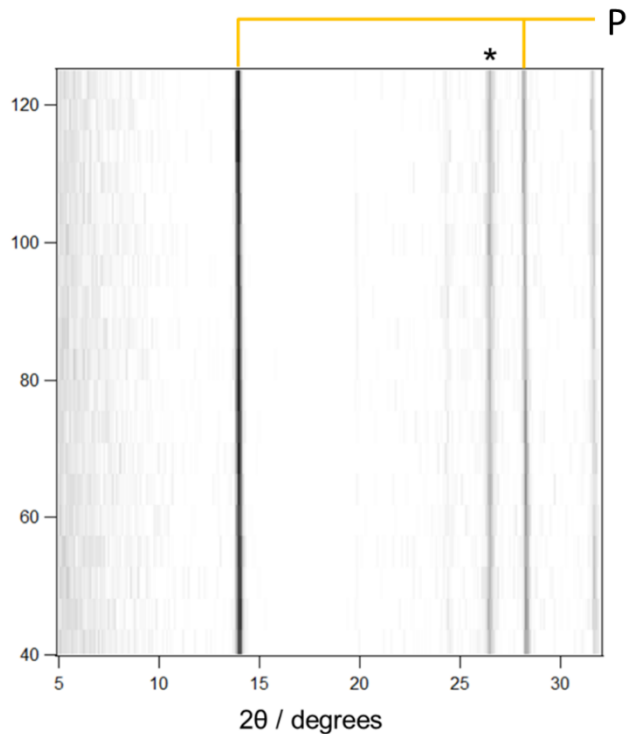


FIG. S8. Without excess MAI in vacuum-deposited MAPbI₃ films, there is no change during annealing in the in situ XRD spectrum. The film maintains the perovskite structure from room temperature up to 125 °C. The star identifies the substrate peak. The horizontal axis is 2θ degrees from XRD, while the vertical axis is temperature in °C, and the value indicates the intensity of the XRD line (dark = more intense).

Reversible Annealing of a Vacuum-Deposited Film with Excess MAI

Perovskite films prepared with excess MAI inside the vacuum chamber are opaque and brown. For comparison, stoichiometric perovskite films are characteristically semi-transparent with a mirror-finished surface. Stoichiometric films are more stable in air (time scale of days). However, films with excess MAI begin to bleach immediately after they are taken out from the chamber and exposed to ambient air (~50% relative humidity); films are transparent within one hour. After air exposure, XRD shows a strong diffraction peak at 11.4° from a water complex

$\text{Pb}(\text{MA})_4\text{I}_6 \cdot 2\text{H}_2\text{O}$.⁶⁻⁸ One transparent sample (FIG. 6a, “As-prepared” sample) was transferred to a N_2 glove box (<0.1 ppm of O_2 and H_2O) and subsequently annealed (FIG. 6a, “105°C/10 s”). The sample recovers its original brownish color. However, as soon as this sample is exposed to air for *ex situ* XRD measurements (time scale of ~10 minutes) the film bleaches again (FIG. 6a, “After XRD”). Most likely, physical incorporation of H_2O , which can be removed by heating above 100°C in N_2 , plays the critical role in this reversible process. We systematically increased the annealing temperature with a constant annealing time of 30 minutes (FIG. 6b). Higher temperatures produced gradual increase in the (110) and (220) diffraction peaks from MAPbI_3 at ~14° and ~28°. However, the 11.4° peak was still predominant until the samples were annealed at 125°C. After annealing at 125°C, the films retained perovskite color and only perovskite peaks were observed in XRD.

XRD Confirmation of Perovskite Structure and Orientation

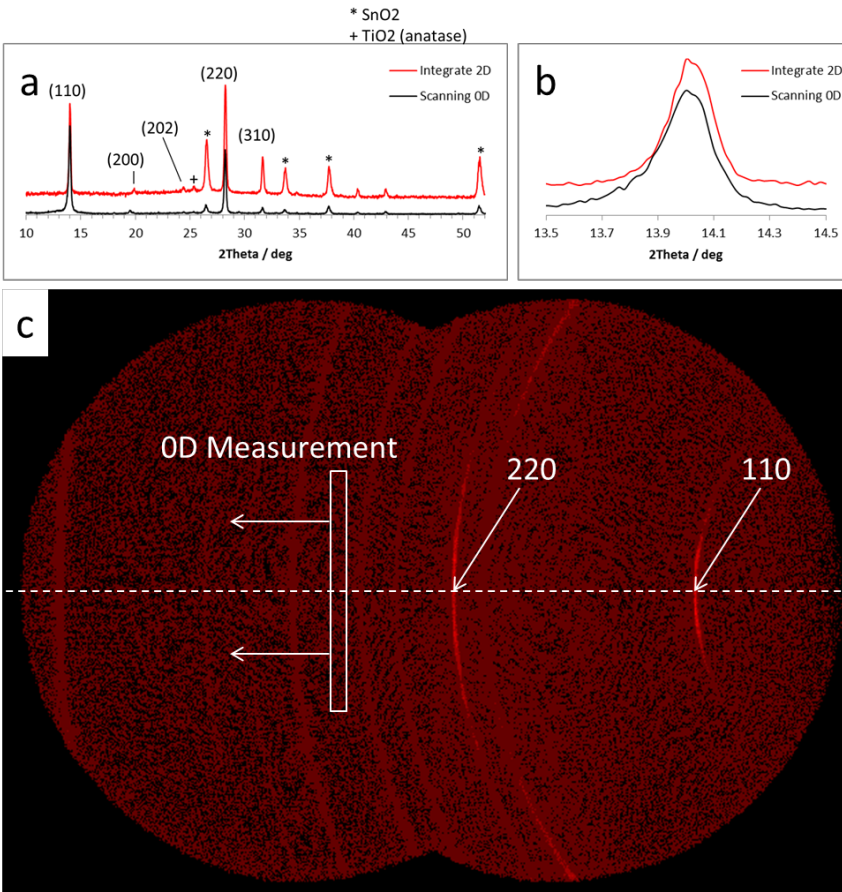


FIG. S9. 2D vs 0D XRD on perovskite film. a) comparison of integrated 2D spectrum vs 0D spectrum. The (202) peak of the perovskite only stands out against the noise in the integrated spectrum. Stars identify substrate peaks from the FTO. Plus signs identify substrate peaks from the TiO_2 layer. c) (110) peak in the integrated 2D spectrum vs 0D spectrum showing broadening and asymmetry in the 0D spectrum. c) 2D XRD spectrum of a perovskite film. White arrows identify the location of the two main perovskite peaks for orienting the viewer. The white box represents the integration area of a 0D measurement that is scanned along the θ axis.

A standard 0D x-ray detector integrates perpendicular to the 2θ plane to enhance signal, but this can lead to distortion and indistinct peaks. With a 2D XRD detector, diffraction rings can be observed and yield additional information about a sample being measured. In a spectrum from a 0D detector, the off-axis portion of the rings will be measured at a lower diffraction angle. As observed in other XRD spectra in this work, the 14° and 28° peaks, respectively from the (110)

and (220) diffraction from a methylammonium lead halide film are clearly visible.⁹ Even when measuring with a 0D detector, the peaks are sharp and more intense than other peaks, which is suggestive of highly-crystalline films that are oriented with the [110] direction orthogonal to the sample surface plane. The 2D spectrum is compared to the 0D spectrum in FIG. S9a. The tetragonal perovskite (202) peak appears only in the integrated 2D spectrum because it is weak and off the 2θ axis, as would be expected for a highly oriented crystal film. If we take a closer look, the (110) peak in the 0D spectrum, as shown in FIG. S9b, is asymmetrical and shifted relative to the symmetrical peak in the 2D spectrum. This is an artifact of the geometry of scanning with a 0D detector (FIG. 11c). These spectra show that the films we prepared are highly ordered and comparable to those in the literature from other groups.

Film Crystallinity and Peak Shifts

We used NaCl to provide a reference point for the broadening of the instrument. We measured the (200) peak of single crystal NaCl at 31.7° in the same powder diffraction mode and with the same conditions that were used in the measurements in this manuscript. The measured full width half max (FWHM) was 0.18° . Polycrystalline films will have broad peaks, in which decreasing grain size will increase the peak width. The integration of the 0D detector will also contribute to broadening that will be accentuated for smaller 2θ angles, as depicted in FIG. S9c. Strained or slightly compressed or expanded grains will also contribute to broadening. Overlapping peaks from other species can also contribute to broadening. If the broadening were only due to grain size and if the grain size were smaller than a few hundred nanometers, then the grain size could be calculated with the Scherrer equation based on peak width.¹⁰ Smaller crystal grains will

produce peaks that broaden as theta increases. Peak positions, d-spacings, and peak widths are presented in Table S1 for OD spectra.

Table S1. Peak positions, associated d-spacings, and peak widths for films with different treatment conditions before and after annealing in air.

	(110)						(220)					
	Initial			Final			Initial			Final		
	2 θ	d	FWHM	2 θ	d	FWHM	2 θ	d	FWHM	2 θ	d	FWHM
2000 fresh	14.1	6.3	0.34	14.0	6.3	0.19	27.7	6.4	0.19	28.2	6.3	0.23
GB closed	14.1	6.3	0.37	14.0	6.3	0.26	27.8	6.4	0.29	28.2	6.3	0.23
GB open	14.1	6.3	0.41	14.0	6.3	0.30	28.3	6.3	0.31	28.3	6.3	0.24
2000 air	14.1	6.3	0.30	14.1	6.3	0.31	27.7 28.3	6.4 6.3	0.50	28.4	6.3	0.32
4000 fresh	14.1	6.3	0.27	14.0	6.3	0.18	28.3	6.3	0.31	28.2	6.3	0.20
4000 air	14.1	6.3	0.29	14.0	6.3	0.19	28.3	6.3	0.32	28.2	6.3	0.20

The significance of some of the peak parameters is apparent. Almost all of the peaks are broader than the NaCl peak, consistent with the polycrystalline films and grains on the order of hundreds of nanometers to microns. Table S1 clearly shows that grain size is not the main source of broadening since the peak width doesn't clearly correlate with theta. In some instances, the (220) peak near 28° is significantly broader than its corresponding (110) peak at 14°. This could be due to an additional shifted D peak, which remains even after some annealing. Narrow peak widths are observed for some samples after annealing. However, the 2 θ angle is lower than would be expected for MAPbI₃. DMA has displaced some of the MA.

One Explanation for the T Phase XRD Peaks

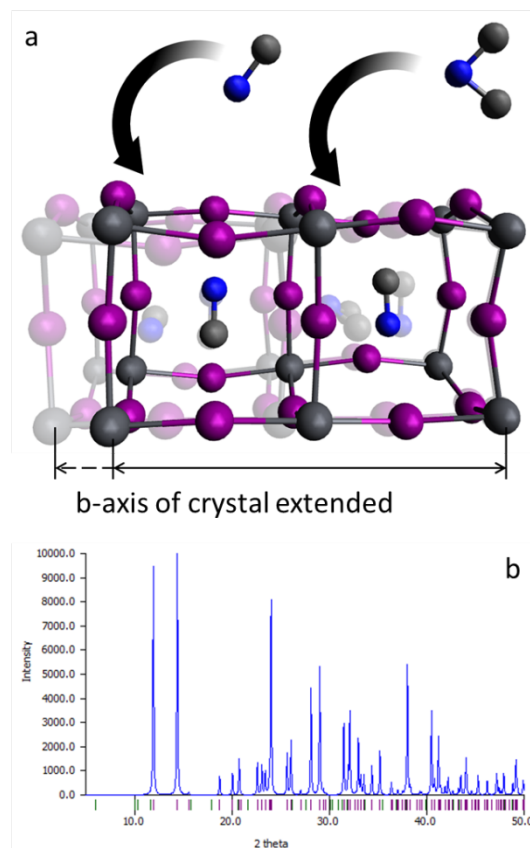


FIG. S10. Illustration of a structure that could produce split peaks at 12.1° and 14.5° in Cu K α XRD. a) If additional alkylammonium cations, e.g. MA or DMA, are inserted into the lattice the b-axis would have to expand. b) A simulated powder XRD spectrum from the expanded structure.

If the MAPbI₃ perovskite structure, P, combines with the (MA)₄PbI₆·2H₂O structure, W, then there would be more than one cation for each PbI₂. If an intermediate of the two structures with 1 < MA < 4 were favored at higher temperatures, it would have a larger unit cell than the stable perovskite structure. One example of a possible structure is shown in FIG. S10a with the associated calculated structure in FIG. 12b.

Perovskites Prepared by Chemical Vapor Deposition

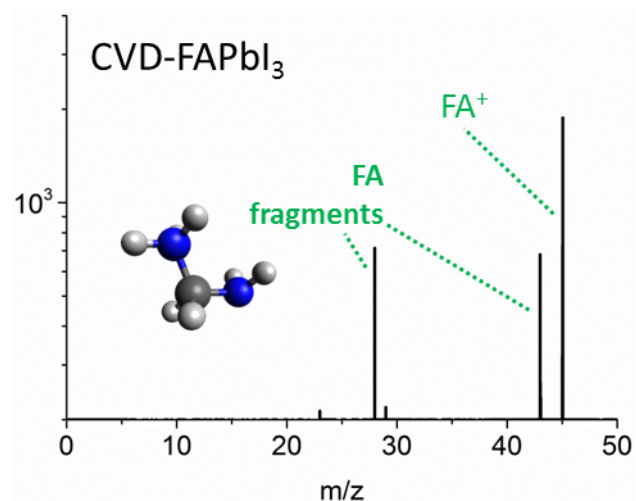


FIG. S11. FAPbI₃ film prepared by chemical vapor deposition (no solvent) to demonstrate that the formamidinium ion doesn't decompose at high temperatures and also to show clear differences due to similar but different cations. No DMA is observed in solvent-free films. In the case of decomposition, NH₃⁺ (m/z = 16) and CH₃NH₂⁺ (m/z = 31) would be likely if formamidinium decomposed chemically rather than fragmenting during analysis; these ions are not present. The small peak at m/z = 23 is from sodium ions that are present at trace levels, but that sometimes appear prominently due to a high ion yield for sodium ions.

For contrast, we also present spectra from a film of a related perovskite, FAPbI₃, which was prepared by chemical vapor deposition (CVD) so solvents were completely avoided. CVD produces very clean films. The cation in FAPbI₃, i.e. formamidinium (FA⁺), is similar in size to dimethylammonium (DMA⁺), but has a distinctly different ionization pattern from that of DMA⁺ or even MA⁺ (FIG. S11). Spectra from FAPbI₃ films are clearly different from those of either SC-MAPbI₃ or Film-MAPbI₃, and these films prepared without solvent only have peaks from a single cation. In CVD, the films are heated to temperatures higher than typical perovskite annealing, yet the formamidinium ion hasn't decomposed. Formamidinium is larger and would be more likely to fragment than methylammonium.

TOF-SIMS Depth Profiling

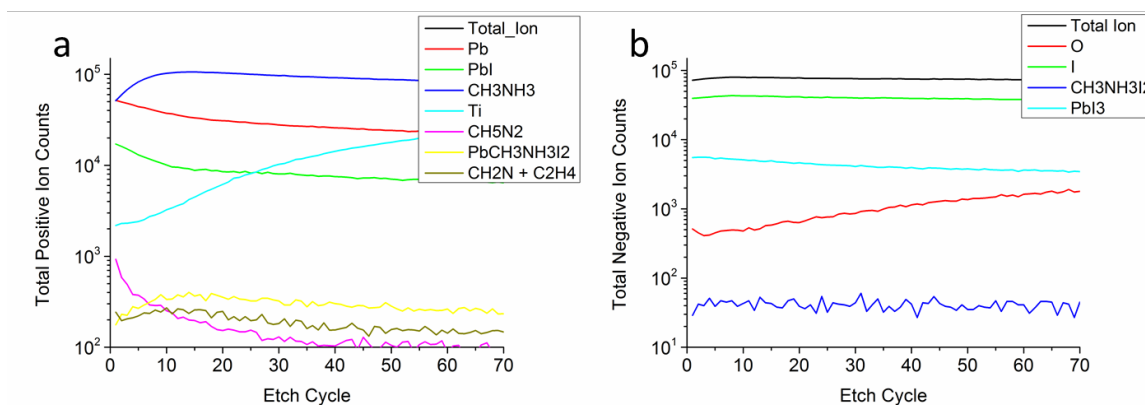


FIG. S12. Depth profiling with TOF-SIMS shows uniform composition through depth. The ion yield of Ti^+ and O^- ions increases roughly an order of magnitude during etching. The yield for other ions is decreases gradually with the increase in TiO_2 .

Depth profiling with TOF-SIMS (FIG. S12) also shows relatively stable composition through the films. The yield of some ions at the surface is different than the bulk by a factor of 2-5x, but much of this is due to the increasing content from mesoporous TiO_2 . Surface analysis of these samples is representative of the bulk. Notably, the ion yield for Pb and PbI are greater near the surface. The MA^+ ion yield is decreases near the surface. This is consistent with MAI leaving the surface during annealing.

XRD of a Film Prepared by the Two-Step Solution Method Using PbI_2 and DMAI

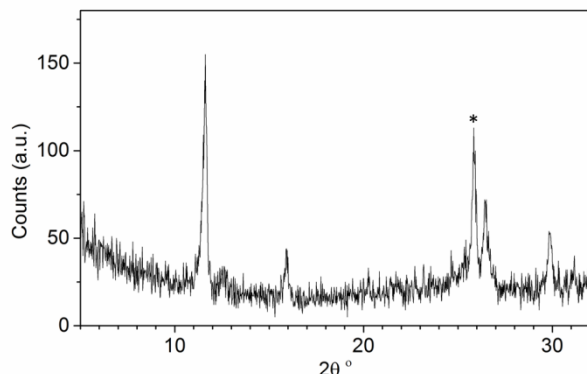


FIG. S13. 2θ - θ XRD on PbI_2 film after exposure to solution of DMAI. The star denotes a SnO_2 substrate peak. DMAI was mixed with PbI_2 in a 1:1 ratio and spin-coated onto a FTO\compact- TiO_2 substrate. The film was clearly translucent, cloudy yellow. Mixing pure DMAI with PbI_2 does not form perovskite and does not readily crystallize.

A film prepared with DMA and PbI_2 was translucent yellow, consistent with a high bandgap. We confirmed that solar cells fabricated from these films produced negligible photocurrent. Based on the XRD, DMA doesn't form a perovskite structure. At high enough concentration as an impurity, DMA will likely disrupt the perovskite structure.

References

- (1) Serp, P.; Hernandez, M.; Richard, B.; Kalck, P. *Eur. J. Inorg. Chem.* **2001**, 2001 (9), 2327.
- (2) Lin, J.-L.; Lin, Y.-C.; Lin, B.-C.; Lai, P.-C.; Chien, T.-E.; Li, S.-H.; Lin, Y.-F. *J. Phys. Chem. C* **2014**, 118 (35), 20291.
- (3) Bipp, H.; Kieczka, H. In *Ullmann's Encyclopedia of Industrial Chemistry*; Wiley-VCH Verlag GmbH & Co. KGaA, 2000.
- (4) Nguyen, H. T.; Nguyen, V. S.; Trung, N. T.; Havenith, R. W. A.; Nguyen, M. T. *J. Phys. Chem. A* **2013**, 117 (33), 7904.
- (5) King, R. B. *J. Am. Chem. Soc.* **1968**, 90 (6), 1412.
- (6) Vincent, B. R.; Robertson, K. N.; Cameron, T. S.; Knop, O. *Can. J. Chem.* **1987**, 65 (5), 1042.
- (7) Wakamiya, A.; Endo, M.; Sasamori, T.; Tokitoh, N.; Ogomi, Y.; Hayase, S.; Murata, Y. *Chem. Lett.* **2014**, 43 (5), 711.
- (8) Christians, J. A.; Miranda Herrera, P. A.; Kamat, P. V. *J. Am. Chem. Soc.* **2015**, 137 (4), 1530.
- (9) Stoumpos, C. C.; Malliakas, C. D.; Kanatzidis, M. G. *Inorg. Chem.* **2013**, 52 (15), 9019.
- (10) Patterson, A. L. *Phys. Rev.* **1939**, 56 (10), 978.